Indian J. Phys. **49**, 227–238 (1975)

X-ray studies on lattice defects of copper-nickel alloys

G. B. MITRA AND T. CHATTOPADHAY

Department of Physics, Indian Institute of Technology, Kharagpur 2

(*Received* 23 *July* 1973, *revised* 9 *October* 1974)

The X-ray diffraction line profiles from nickel, copper and some copper-nickel alloys—cold worked and annealed at different temperatures—have been recorded with the help of a Norelco diffractometer using CuK_α radiation. The background for each line profile thus obtained was determined by the method developed by Mitra & Misra (1966). The line profiles have been corrected for temperature diffuse scattering and for diffuse scattering due to random distribution of guest atoms in host sites and due to difference in sizes of the guest and host atoms. Particle size and strain for cold worked and annealed samples have been found by analysing these line profiles by several existing techniques, *viz.*, integral width, Fourier coefficient and variance methods. In case of nickel and copper-nickel alloys the results indicate two stages in the relief of strain during annealing. Stacking and twinning fault probabilities have been determined by the peak shift and peak asymmetry measurement for the cold worked alloys in the entire concentraion range. Both of these probabilities have been found to reach a maximum at about 40–50 at.% of nickel in copper. The stacking fault energy is found to have an ill-defined minimum at about 30 at.% of nickel.

1. INTRODUCTION

Many important physical properties of crystals are intimately connected with the state of their lattice imperfection. In particular, the strength properties of metals and alloys are found to be dependent on size (Ivernova & Ospenko 1965) and angular misorientation of mosaic blocks (Zhurkov *et al.* 1962), lattice distortion and the stacking fault energy (Noskova & Pavlov 1965). The lower the stacking fault energy the greater will be the distance separating two partial dislocations affecting the process of their dissociation and finally leading to an increase in the strength of the material. Increasing attention has therefore been paid in recent years to the study of the mosaic structure and of the generation of stacking faults and lattice strains on cold working and their removal accompanying the process of recrystallization during annealing in metals and alloys.

The addition of a transition metal like nickel to copper forms a very important alloy system both from the theoretical and industrial point of view. This

system forms a stable face centred cubic disordered solid solution at all compositions. Particle size and lattice strain of this system in cold worked state have been studied by a number of workers (Nakajima & Numakura 1965, Gowsami *et al* 1966) from the analysis of the X-ray diffraction line profiles by the method of integral width and Fourier coefficients. The study of stacking fault probabilities particularly of this system has received a considerable amount of interest. It has been observed that the contribution of transition elements in copper alloys to stacking fault probability is very small compared to that of other elements alloyed with copper (Smallman & Westmacott 1957) and the stacking fault probabilities attain maximum value at about 40–50 at.% of nickel.

The process of recrystallization and removal of lattice strain in pure nickel during annealing have been studied by Michell & Haig (1957) and by Michell & Lovegrove (1960). The results indicate in conformity with those obtained by previous workers (Clarebrough *et al* 1955, 1956) two stages in the relief of strain. The first occurs mainly in the less severely deformed regions without appreciable increase in the apparent particle size. At the second stage all the remaining strain is relieved with an increase in the apparent particle size. Agnihotri & Mitra (1963) have studied the annealing process in pure copper and have found no indication of the two-stage annealing process. However, so far no systematic study of the particle size and lattice strain and their removal due to annealing has been undertaken in copper nickel alloys. The previous workers did not correct the intensity for temperature diffuse scattering and ignored in case of alloys the diffuse scattering due to random distribution of guest atoms in host sites and due to difference in sizes of guest and host atoms. They did not employ any systematic method for selecting a proper background. The recently developed variance method has not been used at all in copper-nickel system. In course of the present investigation an attempt has been made to achieve all these.

2. Experimental Techniques

2.1. *Preparation of the sample*

The samples studied were spectroscopically pure copper, nickel and their alloys (20%, 30%, 40%, 50%, 60%, 80% and 90% of nickel by weight in copper) supplied by M/s. Johnson Matthey & Co., Ltd., (London).

The samples were ground to fine powders filling and were made to pass through a fine sieve. These powdered samples were then annealed at 100°C, 200°C, 300°C, 400°C, 500°C and 600°C. The time of annealing in each case was approximately 2 hours. A portion of each sample was annealed at 800°C for about 12 hours for the study of geometrical broadening of the X-ray diffraction lines. Annealing was carried out in an evacuated chamber placed in an electric furnace whose temperature could be regulated within ± 1°C. The

temperature of annealing was measured with the help of a chromel-alumel thermocouple placed within the evacuated chamber. Annealed powders were mixed with collodion and cakes were made on standard sample holder of an X-ray diffractometer.

2.2. *Study of the distribution of intensity*

The distribution of intensity in the X-ray diffraction lines was determined with the help of a Norelco X-ray diffractometer with ElT counter tubes by point counting method. CuK_α radiations were used for the present investigation. The X-ray generator was made to operate with a full wave rectified high tension supply which was electronically stabilized at 0.1% of the indicated voltage. Counts were taken at angular intervals of 0.01° when a peak was scanned and 0.05° at the background. The angular settings were made manually and counts were taken for 64 seconds at each setting. At the background and at the tail of the intensity distribution, where the counting rate was lower, the time of counting was increased so as to count at least 10,000 at each setting. Thus the statistical fluctuation error was kept at less than 1% level throughout the experiment. The counting rate was corrected for dead time as well as form factor. The dead time of the Geiger counter was determined as 200 -seconds while the form factor was taken as 1.7 since the supply was full wave rectified (Klug & Alexander 1952).

2.3. *Corrections applied to the intensity distribution*

The intensity distribution was corrected for temperature diffuse scattering by the method due to Chipman & Paskin (1959*b*) as modified by Mitra (1965) after a proper choice of the background intensity according to the method developed by Mitra & Misra (1966). For alloys the intensity distribution was further corrected for the diffuse scattering due to random distribution of guest atoms in host sites by the method due to Cochran (1956) and diffuse scattering due to difference in sizes of different atoms by the method of Herbstein *et al* (1956). Geometrical broadening was separated by the method of Stokes (1948) to obtain pure diffraction line profiles.

2.4. *Determination of the particle size and strain*

The particle size and strain in each sample were determined by three methods *viz.*, the method of integral width of Williamson & Hall (1953), the method of Fourier coefficients of Warren & Averbach (1950) and the recently developed method of variance due to Mitra (1964). In case of integral width method the Gaussian distribution of particle size and strain profiles and in Fourier coefficient method Gaussian distribution of strain was considered. ,

2.5. *Determination dislocation density*

Dislocation densities were estimated from particle size and strain values with the help of the method developed by Williamson & Smallman (1956).

2.6. *Determination of stacking and twinning fault probabilities and stacking fault energy*

The stacking fault probability was determined by the method used by Smallman & Westmacott (1957) in which the difference of peak separation (111) and (200) reflections of the sample and the corresponding fully annealed sample is a measure of the stacking fault probability. The twinning fault probability has been measured with the help of the method developed by Warren (1959) using the asymmetry of the line profiles as a measure of the twinning fault probability. The stacking fault energy was calculated from the stacking fault probability and dislocation density by the formula used by Nakajima & Numakura (1965). Shear modulus is assumed to vary linearly in the whole concentration range. The validity of this assumption is supported by the work of Orlov & Fedotov (1966).

3. Results and Discussions

3.1. *Comparative study of the three methods of line profile analysis*

Figures 1, 2, 3, 4, 5 and 6 show the variation of the particle size and strain obtained by three different methods of analysis of X-ray diffraction line profiles with the temperature of annealing for nickel and three copper-nickel alloys. It is seen that these three different methods have yielded widely different values. The reason lies partially in the nature of the quantities actually measured and partially in the relative errors of measurement inherent in the three methods. The methods of Fourier coefficients and variance measure the average thickness

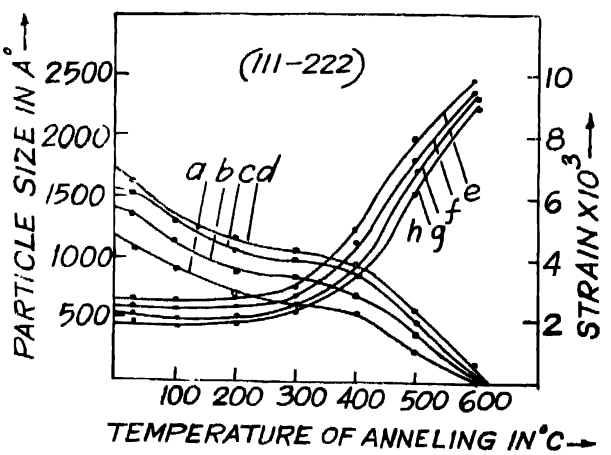

Fig. 1 Variation of the particle size and strain in (111–222) direction with the temperature of annealing as determined by the method of variance, *a*, *b*, *c* and *d* are the strain curves of nickel, 80% Ni in Cu, 60% Ni in Cu and 40% Ni in Cu respectively; *e*, *f*, *g* and *h* are the particle size curves for Ni, 80% Ni in Cu, 60% Ni in Cu and 40% Ni in Cu respectively.

of the coherently diffracting regions in a direction perpendicular to the reflecting plane while the integral width method measures the cube root of the average particle volume. Again while the method of integral width determines the breadth of the strain profile, the other two methods determine the root mean square strain. From the standpoint of measurement there is a wide divergence of assumptions involved. While the method of variance does not make any assumption regarding the nature of either the particle size or the strain profile,

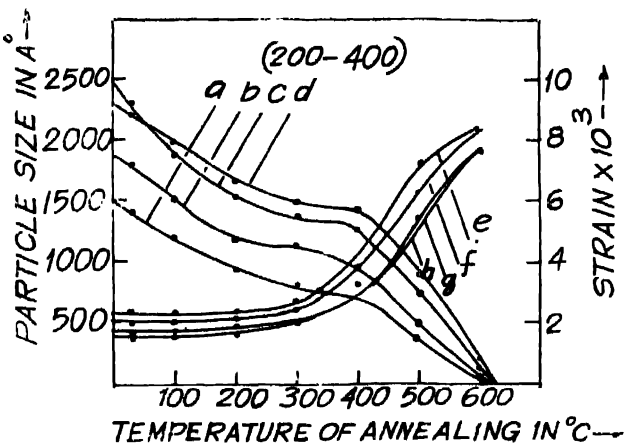

Fig. 2. Variation of particle size and strain in (200–400) direction with the temperature of annealing as determined by the method of variance. *a*, *b*, *c*, *d*, *e*, *f*, *g* and *h* have the same significance as in figure 1.

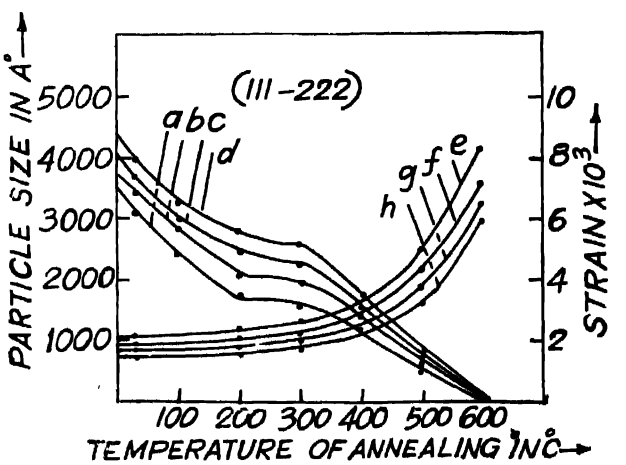

Fig. 3. Variation of particle size and strain in (111–222) direction with the temperature of annealing as determined by the method of integral with, *a*, *b*, *c*, etc. have the same significance as in figure 1.

the method of Fourier coefficients involves assumption of strain profile being of a particular type (Gaussian or Cauchy). The method of integral width involves assumptions regarding both the particle size as well as the strain profiles. It must be noted here that although the method of Fourier coefficients involves assumptions regarding strain only, the particle size measurement is not independent of any assumption. Since the observed line profile is a convolution of the

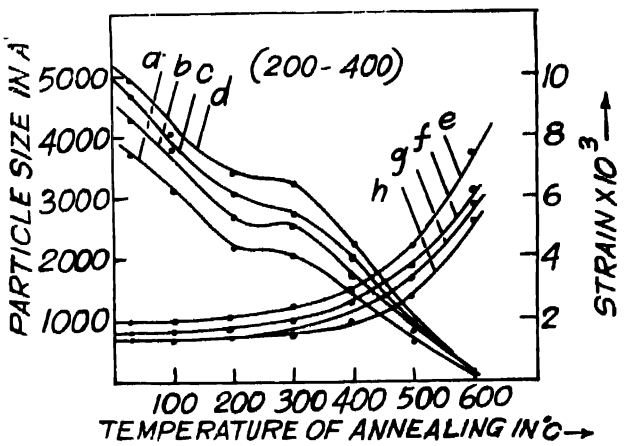

Fig. 4. Variation of particle size and strain in (200–400) direction with the temperature of annealing as determined by the method of integral width. *a*, *b*, *c*, etc. have the same significance as in figure 1

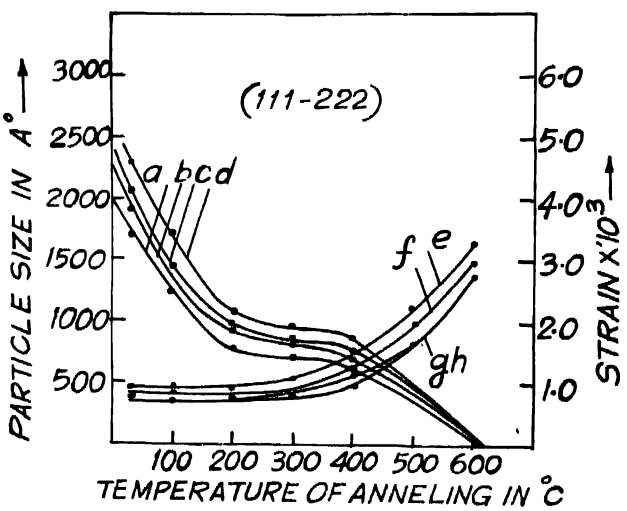

Fig. 5. Variation of particle size and strain in (111–222) direction with the temperature of annealing as determined by the method of Fourier coefficients. *a*, *b*, *c*, etc. have the same significance as in figure 1.

particle size and strain profiles, as soon as the strain profile is assumed to be of a particular type, the particle size profile is also automatically fixed, the observed line profile being what it is. This is why the particle sizes determined on the hypotheses of the strain profile being of Cauchy or Gaussian type are found to

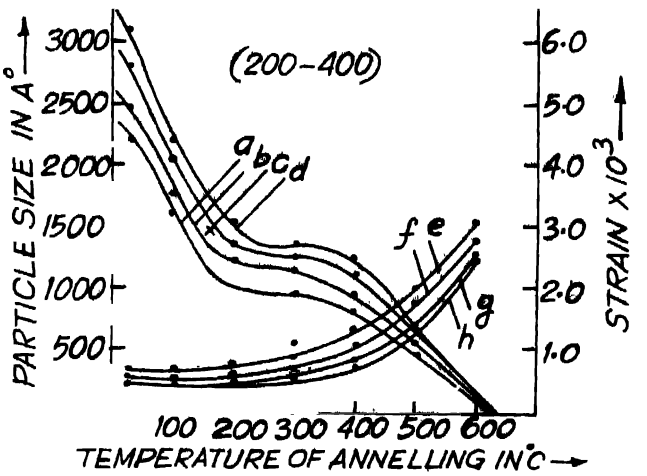

Fig. 6. Variation of particle size and strain in (200–400) direction with the temperature of annealing as determined by the method of Fourier coefficients. *a*, *b*, *c*, etc. have the same significance as in figure 1.

be different. The method of variance suffers from the drawback that equations used in this method have been derived by neglecting certain oscillatory quantities. Systematic errors resulting from this have not yet been estimated. Again both the Fourier coefficient and the variance methods depend on the tails of the line profile which is affected by the particle size distribution. Since integrated intensity is not affected by particle size distribution the measurement involving integral width is independent of particle size distribution. Mitra & Misra (1966) have shown that the incorrect choice of the background level and consequently of the range introduces different errors in different parameters of the line profile. The parameter most affected by the background variation is variance. However, if the background is properly chosen by the method of Mitra & Misra (1966) the variance method is likely to give best results because this method is free from any assumptions regarding the nature of the particle size or strain distribution. Because of this the results of variance method have been used in all subsequent calculations. In this context it can be added that since the previous workers did not apply several corrections mentioned before whereas in the present investigation these have been taken into consideration the results shown here are claimed to be more accurate.

3.2. *Particle size and strain anisotropy*

Table 2 shows the values of t_{111}/t_{100} and s_{100}/s_{111} obtained by the method of Fourier coefficients where t and s are effective particle size and root mean square strain in the direction given by their suffixes along with A and E_{111}/E_{100} values where A in the elastic anisotropic factor given by $A = 2C_{44}/(C_{11}-C_{12})$ and E is the Young's modulus. Table 3 shows the variation of particle size and strain anisotropies obtained by different methods *viz.*, Fourier coefficient, variance and integral width, with the temperature of annealing. In all cases it has been observed that the particle size in (111) direction is more than that in (100) direction and strain in (111) direction is less than that in (100) direction. Anisotropy in particle size obtained may be because of two reasons : one due to real particle size anisotropy and the other due to the presence of faulting because faulting affects different lines differently. It is seen from table 2 that the particle size anisotropy increases with the increase of elastic anisotropic factor. This is quite expected because more faulting occurs in samples with greater elastic anisotropy.

Table 1. Particle size, r.m.s. strain, dislocation densities (obtained by the method of variance), stacking and twining fault probabilities and stacking fault energy of cold worked copper-nickel alloys

Sample	t_{111} Å	$s_{111}\times10^3$	$\rho_t\times10^{-11}$	$\rho_s\times10^{-11}$	$\rho\times10^{-11}$	$\alpha\times10^3$	$\beta\times10^3$	γ in ergs/cm^2
Ni	640	4.25	0.73	7.4	2.23	0.6	0.9	126
Cu 90% Ni	626	5.30	0.76	11.1	2.91	2.0	3.2	45
Cu 80% Ni	602	5.40	0.83	11.5	3.09	3.6	5.9	25
Cu 60% Ni	500	6.40	1.20	16.0	4.39	5.8	9.7	21
Cu 50% Ni	447	6.78	1.50	17.9	5.18	6.9	10.5	20
Cu 40% Ni	450	6.12	1.48	14.5	4.63	7.2	10.4	16
Cu 30% Ni	458	5.97	1 30	12.9	4.10	6.5	8.8	15
Cu 20% Ni	502	5.68	1.19	12.3	3.83	5.5	7.5	16
Cu	523	5.16	1.10	10.1	3.33	3.1	5.4	21

Table 2. Particle size and strain anisotropies of cold worked copper-nickel alloys obtained by the method of Fourier coefficients

Sample	E_{111}/E_{100}	$S_{111}\times10^3$	$S_{100}\times10^3$	S_{100}/S_{111}	t_{111} Å	t_{100} Å	t_{111}/t_{100}	A
Nickel	2.26	3.44	4.40	1.28	450	310	1.45	2.54
Cu 80% Ni	2 29	3.81	4.95	1.30	400	253	1.58	2.84
Cu 60% Ni	2.77	3.83	5.28	1.37	360	213	1.69	3.28
Cu 40% Ni	2.88	3.86	5.60	1.42	348	218	1.60	3.25

Table 3. Variation of the particle size and strain anisotropies obtained by different methods with the temperature of annealing of Cu-Ni alloys

Method	Temperature of annealing °C	Nickel		80% Ni in Cu		60% Ni in Cu		40% Ni in Cu	
		s_{100}/s_{111}	t_{111}/t_{100}	s_{100}/s_{111}	t_{111}/t_{100}	s_{100}/s_{111}	t_{111}/t_{100}	s_{100}/s_{111}	t_{111}/t_{100}
Fourier	30	1.28	1.45	1.30	1.58	1.37	1.69	1.42	1.60
Coefficient	100	1.27	1.42	1.32	1.50	1.40	1.60	1.30	1.55
	200	1.29	1.31	1.31	1.45	1.37	1.55	1.43	1.51
	300	1.30	1.23	1.33	1.30	1.42	1.40	1.40	1.41
	400	1.26	1.16	1.35	1.21	1.41	1.28	1.41	1.30
	500	1.29	1.11	1.30	1.15	1.40	1.15	1.40	1.19
	600	1.27	1.10	1.32	1.06	1.39	1.10	1.39	1.12
Variance	30	1.30	1.12	1.34	1.16	1.42	1.19	1.45	1.18
	100	1.32	1.15	1.35	1.16	1.45	1.18	1.48	1.16
	200	1.34	1.16	1.36	1.15	1.44	1.15	1.43	1.19
	300	1.33	1.10	1.35	1.12	1.43	1.18	1.49	1.15
	400	1.31	1.13	1.38	1.13	1.44	1.17	1.50	1.14
	500	1.32	1.12	1.33	1.14	1.48	1.19	1.46	1.13
	600	1.30	1.14	1.35	1.16	1.39	1.15	1.44	1.15
Integral	30	1.22	1.11	1.26	1.15	1.27	1.11	1.24	1.15
Width	100	1.25	1.12	1.28	1.09	1.26	1.19	1.23	1.14
	200	1.28	1.15	1.29	1.21	1.25	1.12	1.22	1.12
	300	1.26	1.09	1.30	1.18	1.26	1.19	1.26	1.10
	400	1.29	1.10	1.25	1.20	1.25	1.09	1.25	1.09
	500	1.24	1.15	1.23	1.17	1.24	1.15	1.20	1.11
	600	1.21	1.16	1.24	1.16	1.28	1.11	1.28	1.15

That the main contribution to the apparent particle size anisotropy is due to faulting is supported by the results shown in table 3 where it is seen that the apparent particle size anisotropy reduces with the rise of the temperature of annealing and finally attains a low value which may be due to real particle size anisotropy. It is also seen that particle size anisotropy obtained by the method of variance and integral does not change appreciably with the temperature of annealing indicating that faulting affects less in particle size measurement by these two methods. Strain anisotropy may arise in different ways. Stress due to plastic deformation of the crystallites may be anisotropic. This anisotropic stress coupled with elastic isotropy or elastic anisotropy may also give rise to anisotropic strain. According to isotropic stress model the residual microstrain in (*hkl*) direction should be inversely proportional to the Young's modulus in that direction so that $s_{100}/s_{111} = E_{111}/E_{100}$. It is seen from tables 2 and 3 that although s_{100}/s_{111} increases with E_{111}/E_{100} the magnitude of s_{100}/s_{111} is not equal to E_{111}/E_{100}. In fact s_{100}/s_{111} is much less than E_{111}/E_{100}. This rules out

the possibility of isotropic stress in the samples under study. Goswami *et al* (1966) have concluded that the observed anisotropy of strain in copper-nickel alloys may possibly be related to the non-uniform distribution of dislocations and to the stress directionality of stacking faults and dislocations. Previous workers (Smallman & Westmacott 1957, Alder & Wagner 1962) have drawn similar conclusions in other f.c.c. alloys. It is also seen from table 3 that elastic anisotropy does not change appreciably with the temperature of annealing in contrast with the observation by De-Angelis (1964) on explosively loaded copper which have shown that microstrains become more anisotropic on annealing.

3.3. *The annealing process*

Although different methods of line profile analysis have yielded different values of particle size and strain the nature of their variation with the temperature of annealing is almost the same. In nickel and three copper nickel alloys there is clear indication of the two-stage annealing process as seen in figures 1 to 6. This two-stage annealing process was observed by Michell & Haig (1957) in nickel. Previously Clarebrough *et al* (1955, 1956) obtained similar results by a calorimetric study of the stored energy during annealing. In the first stage, relief occurs in the less severely deformed regions without appreciable increase in the apparent particle size. In the second stage, relief occurs in the severely deformed regions which separate the particles. This joins together the smaller particles forming bigger ones. This is the process of recrystallization. The non-monotonic variation of the residual electrical resistivity of copper nickel alloys with temperature of annealing observed by Noskova & Pavlov (1962) may perhaps be attributed to this two-stage annealing process.

3.4. *Variation of the defect parameters with concentration*

Table 1 shows how the particle size t and strain s obtained by the method of variance, dislocation densities ρ_t and ρ_s calculated from the particle size and strain values respectively, stacking fault probability α, twinning fault probability β and stacking fault energy γ of cold worked alloys vary with composition. The variation of particle size and strain with composition is not very remarkable. These two parameters attain maximum and minimum values respectively at about 50% of nickel by weight in copper. The dislocation density also attains maximum values at the same percentage. It is seen that the dislocation densities (and hence stacking fault energies) calculated from particle size and strain values are widely different. This implies that the simplified model of Williamson & Smallman (1956) which assumes $F = 1$ and $n = 1$, where F is the intersection factor of dislocation and n is the number of dislocations per block face is not valid because according to this model dislocation densities calculated from particle size and strain values should have been equal. In the absence of extensive

piling up and polygonization a lower limit to ρ given by $\rho = (\rho_s \rho_t)^{\frac{1}{2}}$ can be determined. These are also shown in table 1 along with stacking fault energies calculated from these values. The stacking and twinning fault probabilities are found to attain a maximum (figure 7) at about 40–50% of nickel by weight in copper. The stacking fault energy versus nickel concentration curve has an ill-defined minimum at approximately 30% of nickel by weight in copper. The twinning fault probabilities are found to be more than stacking fault probabilities at all compositions in agreement with the results obtained by Goswami *et al* (1966) although the actual values do not agree with those obtained by them. This may be because of the greater uncertainty in the measurement of this parameter. The possibility of twinning faults is confirmed from the observations of twin abundance in a number of different alloys by Irving *et al* (1964-65). Values of the stacking fault probabilities obtained in course of the present investigation agrees well with those obtained by Henderson (1963-64) and Goswami *et al* (1966). Nakajima & Numakura (1965) have obtained higher values.

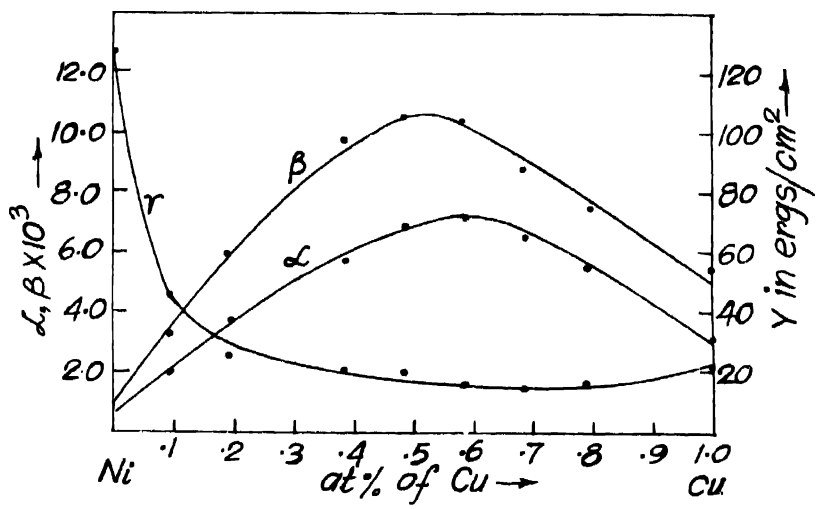

Fig. 7. Variation of stacking and twinning fault probabilities and stacking fault energy of copper-nickel alloys with concentration.

The fact that the addition of transitional elements in copper does not cause a large increase in the stacking fault probability and the observed maximum of stacking fault probability versus concentration curve at about 40–50% of nickel in copper have been the subject of much recent discussions. The works of Davies & Cahn (1962) suggest that the electron/atom ratio, the valency of the solute atom, size and period difference between the solute and the solvent atoms and the relative stabilities of the f.c.c. and h.c.p. phases are responsible for the stacking fault probability of an alloy which in turn is closely related with the stacking

fault energy. In copper nickel system, however, the solute and the solvent atoms are in the same period, their size difference is very small and the face-centred cubic phase is stable at all compositions. Hence the stacking fault probability and energy will be mainly governed by the electron concentration, and the interactions through the incompletely filled 3*d* shells of the transitional solute nickel.

References

Adler R. P. I. & Wagner C. N. J. 1962 *J. Appl. Phys.* **33**, 3451.

Agnihotri O. P. & Mitra G. B. 1963 *Phil. Mag.* **8**, 1161.

Chipman D. R. & Paskin A. 1959*b* *J. Appl. Phys.* **30**, 1998.

Clarebrough L. M., Hargeaves M. E. & West G. W. 1955 *Proc. Roy. Soc.* **A232**, 252.

Clarebrough L. M., Hargeaves M. E. & West G. W. 1956 *Phil. Mag.* **1**, 528.

Cochran W. 1956 *Acta Cryst.* **9**, 259.

Davies R. G. & Cahn R. W. 1962 *Acta Met.* **10**, 621.

De Angeles R. J. 1964 Ph.D. Thesis, North Western University.

Goswami K. N., Sengupta S. P. & Quader M A. 1966 *Acta Met.* **14**, 1559.

Henderson B. 1963-64 *J. Inst. Metals* **92**, 55.

Horbstein F. H., Borie B. S. & Averbach B. L. 1956 *Acta Cryst.* **9**, 466.

Irving C., Miodownick A P. & Towner J. M. 1964-65 *J. Inst. Metals* **93**, 360.

Ivoronova V. I. & Osipenko N. N. 1965 *Fiz. Metal. Metalloved.* **20**, 417.

Klug H. P. & Alexander L. E. 1952 *X-ray Diffraction Procedures* (New York, John Wiley), p. 223.

Michell D. & Haig F. H. 1957 *Phil. Mag.* **2**, 15.

Michell D. & Lovegrove E. 1960 *Phil. Mag.* **5**, 499.

Mitra G. B. 1964 *Acta Cryst.* **17**, 765.

Mitra G. B. 1965 *Brit. J. Appl. Phys.* **16**, 77.

Mitra G. B. & Misra N. K. 1966 *Brit. J. Appl. Phys.* **17**, 1319.

Nakajima K. & Numakura K. 1965 *Phil. Mag.* **12**, 361.

Noskova N. I. & Pavlov V. A. 1962 *Fiz. Metal. Metalloved* **14**, 899.

Noskova N. I. & Pavlov V. A. 1965 *Fiz. Metal. Metalloved* **20**, 428.

Orlov A. F. & Fedotov S. G. 1966 *Fiz. Metal. Metalloved* **22**, 137.

Schindler A. I. & Pugh E. M. 1953 *Phys. Rev.* **89**, 295.

Seeger A. 1957 *Dislocation and Mechanical Properties of Crystals* (New York, and London, John Wiley), p. 243.

Smallman R. E. & Westmacott K. H. 1957 *Phil. Mag.* **2**, 669.

Stokes A. R. 1948 *Proc. Phys. Soc.* **61**, 382.

Warren B. E. & Averbach B. L. 1950 *J. Appl. Phys.* **21**, 595.

Warren B. E. 1959 *Prog. Metal Phys.* **8**, 147.

Williamson G. K. & Hall W. H. 1953 *Acta Met.* **1**, 22.

Williamson G. K. & Smallman R. E. 1956 *Phil. Mag.* **1**, 34.

Zhurkov S. N., Betekhtin V. I. & Slutskor A. I. 1962 *Fiz. Metal. Metalloved* **13**, 718.